



Assessment with remotely sensed soil moisture products and ground-based observations over three dense network

Gang Yang¹ · Peng Guo¹ · Xican Li¹ · Hong Wan^{1,2} · Chunhong Meng¹ · Bo Wang¹

Received: 6 November 2019 / Accepted: 4 March 2020 / Published online: 16 March 2020
© Springer-Verlag GmbH Germany, part of Springer Nature 2020

Abstract

Soil moisture (SM) is a key variable in hydrological processes, bio-ecological processes, and biogeochemical processes. Long-term observations of soil moisture over large areas are critical to research on flooding and drought monitoring, water resource management, and crop yield forecasts. In this paper, Fengyun (FY3B and FY3C) SM products, Japan Aerospace Exploration Agency (JAXA) SM products from the Advanced Microwave Scanning Radiometer 2 (AMSR2), the Land Parameter Retrieval Model (LPRM) AMSR2 L3 SM products, the Version 2 (v2) global land parameter data record (LPDR) of SM products, Soil Moisture Ocean Salinity (SMOS) Centre Aval de Traitement des Données SMOS (CATDS) L3 SM products, the Soil Moisture Active Passive (SMAP) passive L3 SM products and the European Space Agency (ESA) Climate Change Initiative (CCI) SM products were evaluated using the ground-based observations in the Little Washita, Fort Cobb and Yanco networks. Long-time series comparison between measured and satellite products was conducted to evaluate the overall performance of FY3 series satellites SM products. Bias (mean bias), R (correlation coefficient), RMSE (root mean square error) and ubRMSE (unbiased root mean square error) were calculated to explore the agreement between satellite products and in-situ measurements. Taylor diagrams were used to compare the performance of various satellite products. The result showed that (1) FY3B, FY3C and LPRM AMSR2 ascending and descending products had an obvious overestimate with in-situ soil moisture in three networks. (2) JAXA AMSR2 ascending and descending products had considerable underestimation in three networks. (3) The validation result of SMOS ascending and descending products over the three networks was satisfactory, with a rather high correlation than other X-band products. (4) The validation result of SMAP ascending and descending products outperformed the other products over the Little Washita and Fort Cobb networks. (5) The ESA CCI product had the lowest values of RMSE and ubRMSE than the other products in the Yanco network, revealing the effectiveness of merging active and passive soil moisture products. (6) The LPDR descending SM products had better performance than the LPDR ascending SM products in the LW and FC networks.

Keywords Soil moisture · FY3B · FY3C · JAXA AMSR2 · LPRM AMSR2 · SMOS · SMAP · ESA CCI · LPDR · Assessment

Introduction

Soil moisture (SM) is an active part of the terrestrial water cycle. It is the key variable of hydrological process, bio-ecological process and biochemical and plays an important

role in surface water evaporation and seepage (Daly and Porporato 2005; Douville and Chauvin 2000; Schmugge et al. 1974). Long-term observation of large area soil moisture is important for drought and flood checking, water resources management and crop yield prediction (Saini et al. 2016; Bolten et al. 2009). Therefore, accurate measurement of global or continental soil moisture is of great practical significance.

Traditionally, surface soil moisture has been obtained through different measurement techniques such as weight sampling and TDR sensor (Blonquist et al. 2005), although it is possible to accurately measure the soil moisture information of a single point, but it is difficult to provide the spatial and temporal variability soil moisture information at large scales. Currently, the microwave remote sensing is considered as the best way to monitor soil moisture since it can provide

Communicated by: H. Babaie

✉ Peng Guo
guopeng@sdau.edu.cn

¹ College of Information Science and Engineering, Shandong Agricultural University, NO.61 Daizong Street, Taian 271018, China

² Aerospace Information Research Institute, Chinese Academy of Sciences, Beijing 100101, China

the absolute soil moisture at large scale with high temporal. Since the late 1970s, a series of active and passive microwave satellites or sensors have been successfully used for soil moisture monitoring both spatially and temporally. These include the Advanced Space Scatterometer (ASCAT) (Wagner et al. 2013), the Advanced Microwave Scanning Radiometer (AMSR-E) (Njoku et al. 2003), the Spaceborne Polarized Microwave Radiometer WindSat, AMSR2 (the Advanced Microwave Scanning Radiometer 2) (Imaoka et al. 2012), the Soil Moisture and Ocean Salinity (SMOS) of European Space Agency (ESA) (Kerr et al. 2010), the Chinese Fengyun 3B (FY3B) and 3C satellite (FY3C) (Yang et al. 2012), and the latest Soil Moisture Active Passive (SMAP) (Entekhabi et al. 2010) launched by National Aeronautics and Space Administration (NASA). On this basis, a variety of microwave satellite soil moisture products have been freely released to the public by various agencies around the world, such as the ESA's SMOS SM product, the AMSR2 SM products released by the Japan Aerospace Exploration Agency (JAXA), and the FY3B and FY3C SM products issued by China National Meteorological Center. Additionally, the European Space Agency (ESA) developed the first multi-satellite combined soil moisture dataset supported by the Climate Change Initiative (CCI) program to meet the requirement for long-term and globally remotely sensed soil moisture record, i.e., the ESA CCI soil moisture product (Dorigo et al. 2017).

It's very important to understand the spatio-temporal error characteristics and limitations of various satellite soil moisture products, as it can help researches use the optimal product and improve the algorithm. Many researches have carried out satellite SM products accuracy verification work and have shown that different product has different error characteristics and limitations under different environmental conditions (Cui et al. 2018; Chen et al. 2017; Cui et al. 2017; Jackson et al. 2010; Liu et al. 2018; Li et al. 2018; El Hajj et al. 2018; Parinussa et al. 2014; Yee et al. 2017; Zeng et al. 2015; Zhang et al. 2017;). Cui et al. (2017) validated SMOS, SMAP, and four AMSR2 soil moisture products in the Genhe area of China where they found that the quality of the SMOS was superior to the AMSR-2 products and the JAXA product had a constant bias of $0.089\text{--}0.099\text{ m}^3\text{ m}^{-3}$. Cui et al. (2018) compared eight satellite-based soil moisture products (i.e., SMAP, SMOS, JAXA, LPRM, ESA CCI, FY3B) over two dense network regions at different spatial scales, and found that FY3B soil moisture outperformed the other products in the REMEDHUS network region, with an ubRMSE of $0.025\text{ m}^3\text{ m}^{-3}$. Zeng et al. (2015) attended a full validation of mainstream soil moisture products (i.e., JAXA, AMSR2, LPRM, ASCAT, NASA, SMOS, and ERA-Interim) over the Tibetan Plateau, and proved that the AMSR2 products underestimate the ground measurements at most of the time. Yee et al. (2017) evaluated the performance of different SM products from AMSR2 and SMOS against the most

representative stations within the Yanco study area and found that morning retrieval of SMOS was superior to evening retrievals. Parinussa et al. (2014) first compared the soil moisture products derived from the FY3B official algorithm against in-situ measurements.

Although many researchers have analyzed the degree of accuracy among different SM products, very limited studies examine the quality of the Chinese FY3B and FY3C SM products, especially in Australia. Multi-satellite SM combined provides a way for overcoming the limitations of an individual product. The FY SM products have a long-term SM record starting from July 2011, which is an important data source for SM combined. Consequently, in this study, FY3B SM products (including ascending and descending data, separately named FY3B_A and FY3B_D), FY3C SM products (including ascending and descending data, separately named FY3C_A and FY3C_D), SMOS SM products (including ascending and descending data, separately named SMOS_A and SMOS_D), SMAP SM products (including ascending and descending data, separately named SMAP_A and SMAP_D), JAXA AMSR2 SM products (including ascending and descending data, separately named JAXA AMSR2_A and JAXA AMSR2_D), LPRM AMSR2 SM products (including ascending and descending data, separately named LPRM AMSR2_A and LPRM AMSR2_D), the LPDR v2 (including ascending and descending data, separately named LPDR_A and LPDR_D) and ESA CCI SM products were separately assessed over three dense in-situ networks in the southwestern Oklahoma and Southeastern Australia. These satellite SM products are mainstream soil moisture products and there are many years of soil moisture monitoring data to better study satellite performance. The objective of this study was to explore the global applicability and accuracy of the FY series satellite SM products and compare the performance of the FY series satellite SM products with the X-band and L-band SM products. In the following section, the networks and the SM products used for this study are briefly introduced. Third section describes the method for the evaluation of the products. The results are then presented in fourth section. Fifth section discusses the possible explanations for the results. Finally, some conclusions of the study are summarized in sixth section.

Data

Study area and in-situ soil moisture data

To assess the suitability of global soil moisture products over different continents, three networks located in the two different continental regions were used to separately evaluate the performance of satellite SM products: Agricultural Research Service (ARS) networks in southwestern Oklahoma and

Yanco network in the Australia. There are two reasons for choosing these three observation networks as our study area. Firstly, these three observation networks provide high-quality and dense in-situ measurements, which can reduce the problem of mismatch between ground-related point scales and satellite pixels. It is well known that the high spatial variability of soil moisture makes the observations of a single site not representative of the retrievals of a satellite pixel. Fortunately, dense and continuous in-situ measurements can be provided in the three observation domains, so the average measurement results from multiple sites can minimize the inherent spatial scale problems. Secondly, the ARS and Yanco networks have different land cover. Although the climate is similar, due to the opposite rhythm of temperature change between the northern and southern hemispheres, the seasons are quite opposite. It enables a more reliable assessment of satellite SM products. The details of the three networks are described below.

(1) ARS Network: The ARS operates two networks in southwestern Oklahoma; Little Washita (LW) network and Fort Cobb (FC) network. The LW experimental area has been used for soil moisture research for a long time (Leroux et al. 2013; Collow et al. 2012; Jackson et al. 2010), and its observation data has verified the accuracy of various satellite SM products. The LW network is located in the southwestern part of Oklahoma in the Great Plains of the United States. It has an area of approximately 610 km² and a semi-humid climate with an average annual precipitation of 750 mm. The land use type is mainly grassland. There are currently 20 monitoring stations in the LW experimental area to provide monitoring data, and the stations are separated by about 5 km. The FC network was deployed in 2005 and currently has 15 stations that can monitor data. The surface of the ARS hydrological monitoring network measures surface soil moisture (5 cm, 25 cm, and 45 cm), soil temperature (5 cm, 10 cm, 15 cm, 30 cm) and daily rainfall data every 5 min. In this study, the 5 cm depth measurements and daily rainfall were used to evaluate satellite SM products. The data can be downloaded freely (<http://ars.mesonet.org/>).

(2) Yanco Network: Yanco network is one of the OzNet hydrological monitoring network, which is within the Murrumbidgee River catchment in New South Wales, Australia (Fig. 1). The Yanco network is a 60 km × 60 km square area to the south and west of the Yanco Research Station. It is gently sloping and contains much of the Coleambally Irrigation District. There are 37 soil moisture sites distributed across the Yanco network. All of the sites can provide soil moisture at 0–5 (or 0–8), 0–30, 30–60, and 60–90 cm depths. Only 13 stations can provide daily rainfall. Considering the missing data of some stations, the data (Smith et al. 2012) provided by 32 stations was used in this study. The measurements of 0–5 cm depth and daily rainfall was chose to evaluate satellite SM products. The data can be acquired freely (<http://www.oznet.org.au/>).

Satellite soil moisture products

FY3B and FY3C soil moisture products

FY3B and FY3C satellites were successfully launched on November 4, 2010 and September 23, 2013, respectively. Both the FY3B and FY3C satellites are equipped with a microwave radiation imager (MWRI), a 10-channel five-band passive radiometer system that measures horizontal and vertical polarization brightness temperatures from 10.65 GHz to 89 GHz. FY3B's ascending time is about 13:30 in the afternoon and the descending time is 1:30 in the morning. FY3C's ascending time is about 22:30 in the afternoon and the descending time is about 10:30 in the morning.

At present, the soil moisture products released by FY3C include: MWRI soil moisture daily product, MWRI soil moisture monthly product and MWRI soil moisture product, while FY3B only has MWRI soil moisture daily product. This article uses FY3B and FY3C daily soil moisture products, including ascending and descending, which can be downloaded from the National Satellite Meteorological Center (<http://satellite.nsmc.org.cn/PortalSite/Default.aspx>). Both FY3B and FY3C soil moisture products use EASE-Grid projection with a grid resolution of 25 km, and the soil moisture product data format is HDF5. In the current FY3 official algorithm, soil moisture is retrieved using dual-polarized X-band 10.7 GHz channel brightness temperature data. For the bare soil area, the parameterized surface emissivity model QP inversion model is used (Shi et al. 2005), and for the vegetation coverage area, the empirical relationship between the normalized difference vegetation index and the vegetation water content is used to estimate the vegetation optical thickness to correct the vegetation (Liu et al. 2013).

SMOS soil moisture products

The Soil Moisture Ocean Salinity satellite, successfully launched on 2 November 2009, by the ESA, is currently the only one in the world that can simultaneously observe changes in SM and salinity (Kerr et al. 2012). The SMOS can obtain global coverage data every three days with ascending and descending orbits at 6:00 am local solar time and 18:00 pm local solar time, respectively. In the SMOS retrieval algorithm, multi-angular brightness temperature observations are used to retrieve soil moisture and vegetation optical depth simultaneously, by minimizing the difference between the observed and estimated brightness temperature. The radiation transmission model selected for SMOS soil moisture retrieval is the L band Microwave Emission of the Biosphere (L-MEB) model (Wigneron et al. 2007). The SMOS products used in this study were the Level 3 Soil Moisture (L3, Version 3.00) products from the Centre National d'Etudes Spatiales and the Centre Aval de Traitement des Données SMOS. The SMOS

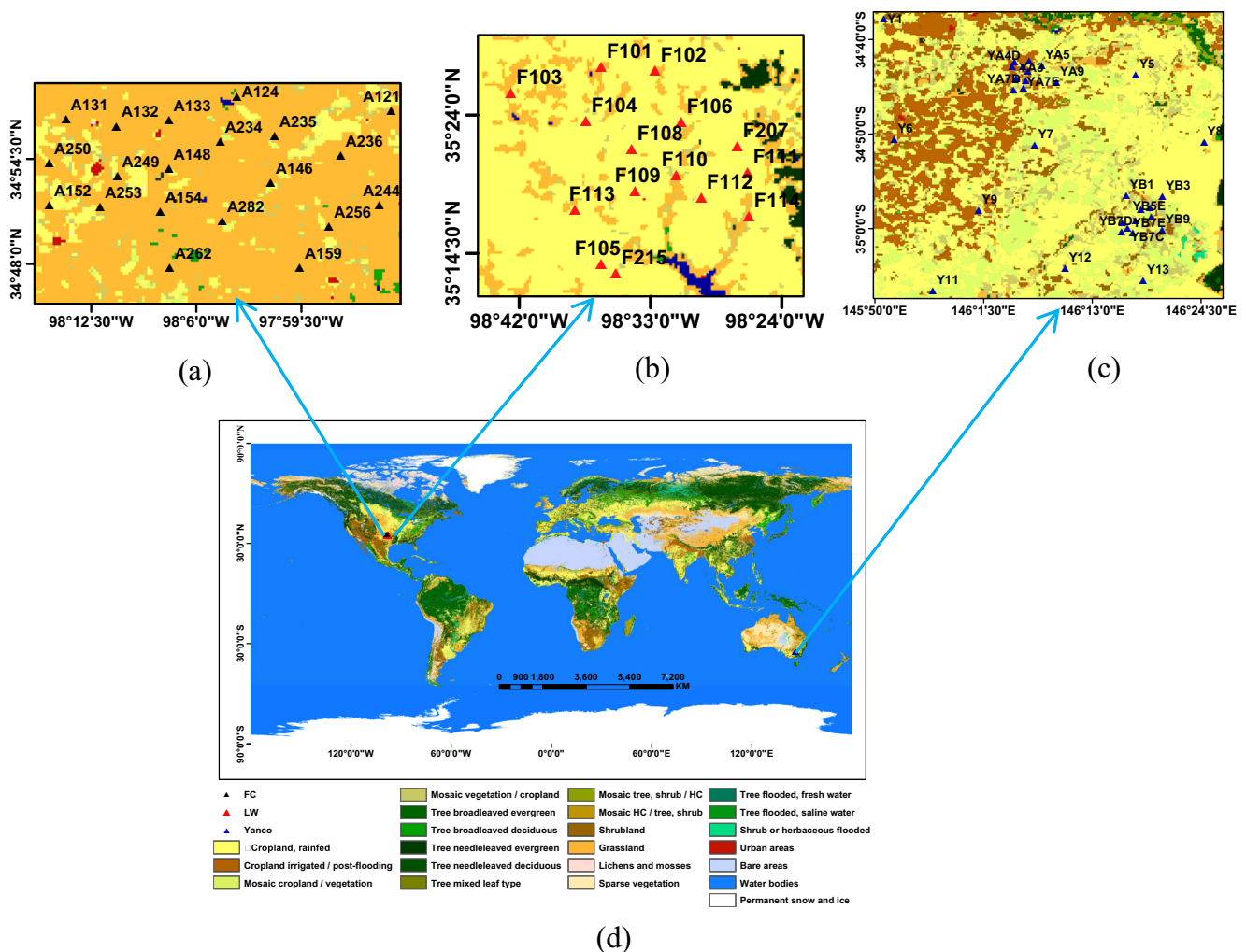


Fig. 1 Location of the ARS and Yanco networks, the distribution of the corresponding stations: **a** LW network, **b** FC network, **c** Yanco network and **d** the legend of the color map denotes the Moderate Resolution

Imaging Spectroradiometer (MODIS) International Geosphere Biosphere Program (IGBP) global land cover classes at 300 m spatial resolution (<http://maps.elie.ucl.ac.be/CCI/viewer/>)

SM product is available at <https://www.catds.fr/Products/Products-access>. The SMOS measurements used in this study were filtered by two conditions: (i) the Data Quality Index (DQX) > 0.06, and (ii) the probability of radiofrequency interference (RFI_Prob) > 0.2 (Cui et al. 2018, 2017;)

AMSR2 soil moisture products

AMSR2 is a single-mission instrument onboard the Global Change Observation Mission 1—Water (GCOM-W1) satellite that was launched by the Japan Aerospace Exploration Agency (JAXA) in May 2012. The data are available beginning in August 2012. The available soil moisture product was provided by the JAXA Earth Observation Research Center (EORC) from both the ascending (13:30 local time) and descending (1:30 local time) overpasses. The soil moisture

products used in the study were downloaded from the GCOM-W1 Data Service Center (<https://gportal.jaxa.jp/gpr/>). The JAXA AMSR2 provides soil moisture product at two spatial resolutions, i.e., 0.1° and 0.25°. In this study, the JAXA AMSR2 Level 3 SM product with a grid resolution of 0.25° was used. The algorithm of the JAXA AMSR2 SM product adopts a lookup table method and multichannel (10–36 GHz) brightness temperatures to estimate surface soil moisture. Two soil moisture products derived from AMSR2, i.e., the JAXA and LPRM SM products, are released to the public, and therefore used in the study.

The spatial resolution of LPRM AMSR2 SM product is 0.25°, which is retrieved using the LPRM algorithm (Owe et al. 2008). Similar to the FY3B algorithm, LPRM uses Ka-band V-polarized bright temperature values to estimate the surface temperature (Holmes et al. 2009). Using the

microwave polarization difference index (MPDI), through non-linear iteration, both soil moisture and vegetation optical thickness are obtained. For LPRM, both C-band and X-band observations are used to obtain soil moisture. Njoku et al. (2005) found that C-band microwave observations were severely affected by radio frequency interference (RFI) in most parts of the United States. Therefore, to minimize uncertainty from RFI, we use LPRM's X-band soil moisture products. LPRM SM product is available from the Goddard Geoscience Data and Information Service (GES DISC) (<https://gcmd.gsfc.nasa.gov/>).

SMAP soil moisture products

SMAP with L-band radar and L-band radiometer was launched by NASA in January 2015. The local equatorial overpass time of the SMAP satellite is 18:00 P.M. (ascending) and 6:00 A.M. (descending). SMAP provides a total of four remotely-sensed soil moisture products, which are the passive, the active, the active-passive, and the enhanced passive soil moisture product. Since the SMAP radar ceased operations in July 2015, resulting in only a short period of time with the active and active-passive soil moisture products, therefore, the SMAP passive SM product, which have run from 31 March 2015 to the present, was used for evaluation in this study. The SMAP product can be downloaded freely from the National Snow and Ice Data Center (NSIDC) (<https://nsidc.org/data/smap/smap-data.html>).

The daily SMAP passive level-3 product (version 6) with a spatial resolution of 36 km, generated on EASE-Grid 2.0, was used in this paper. The V-pol single channel algorithm (SCA-V) is the current baseline retrieval algorithm of the SMAP passive soil moisture product (Chan et al. 2016). For SCA-V, soil moisture can be retrieved from SMAP brightness temperature by the following five steps. First, the brightness temperature is normalized to apparent emissivity, by using surface temperature auxiliary data derived from the Goddard Earth Observing System (GEOS)-5 model to remove the effects of soil and vegetation physical temperature. Second, the vegetation effects are corrected using MODIS normalized difference vegetation index (NDVI) auxiliary data. Third, the soil surface roughness effects are corrected by applying a semi-empirical roughness model, known as the H_p model (Choudhury et al. 1979). Fourth, the Fresnel equations are adopted to convert emissivity to soil permittivity. Finally, soil permittivity is converted to soil moisture, by using the Mironov dielectric model (Mironov et al. 2009).

ESA CCI soil moisture products

ESA CCI Soil Moisture Product (formerly known as ECV Soil Moisture Product) combines active and passive microwave soil moisture retrieval values, a long-term global daily soil moisture record established by the European Space Agency (ESA) With a spatial resolution of 0.25° . In our research, we used the newly released ESA CCI v04.5 soil moisture product, which spans more than 38 years (from November 1978 to December 2018) ESA CCI SM consists of three data sets, including active, passive and active-passive fusion soil moisture products. Active soil moisture products are obtained from microwave scatterometers (SCAT and ASCAT) using change detection methods (TU Wien WARP v5.5). Passive soil moisture products are obtained from a variety of microwave radiometer products. These microwave radiometers include SSM / I (Scanning Multichannel Microwave Radiometer Special Sensor Microwave Imager), TMI (Tropical Rainfall Measuring Mission Microwave Imager), AMSR-E, WindSat, AMSR-2 and SMOS, the algorithm used is LPRM. ESA CCI is a comprehensive product that combines active and passive soil moisture. In this study the ESA CCI active and passive SM product was used.

LPDR v2 soil moisture products

The Version 2 global land parameter data record was generated using calibrated microwave brightness temperature records from the Advanced Microwave Scanning Radiometer for EOS (AMSR-E) on the NASA EOS Aqua satellite, and the Advanced Microwave Scanning Radiometer 2 (AMSR2) sensor on the JAXA GCOM-W1 satellite (Du et al. 2017). The LPDR data files are provided in GeoTIFF (.tif) format. The data are projected into 25 km global EASE-Grid (v1) format. The Version 2 algorithm was derived based on the general framework of the Version 1 algorithm (Jones et al. 2010) and later algorithm revisions (Du et al. 2014, 2016). More details of the description of the LPDR v2 algorithms and changes can be found in (Du et al. 2017). The data can be downloaded freely from the National Snow and Ice Data Center (NSIDC) (<https://nsidc.org/data/nsidc-0451>).

Methods

In this study, in-situ measurements from dense stations in both the ARS and Yanco networks were used to examine the performance of seven satellite SM products, including, the SMOS SM product at 25 km, the JAXA AMSR2 SM product at 0.25° , the FY3B SM product at 25 km, the FY3C SM product at 25 km, the LPRM AMSR2 SM product at 0.25° ,

the ESA CCI SM product at 0.25° , the SMAP passive SM product at 36 km. We calculate that the average temperature of all stations is higher than 0° during the whole observation period, so the influence of frozen soil was not considered in this study. We compared the average measured SM at all stations in each observation network with the average of all satellite grids in each observation network. When comparing the measured soil moisture with the satellite SM products, we classified the ESA CCI SM products into L-band in order to facilitate the comparison.

The error metrics we used in the study include Bias (mean bias), the root mean square error (RMSE), the correlation coefficient (R), the bias and the unbiased RMSE (ubRMSE) (Cui et al. 2017), which are defined as follows:

$$\text{RMSE} = \sqrt{E\langle(\theta_s(t) - \theta_g(t))^2\rangle} \quad (1)$$

$$\text{Bias} = E\langle(\theta_s(t) - \theta_g(t))\rangle \quad (2)$$

$$\text{ubRMSE} = \sqrt{E\langle((\theta_s(t) - E\langle\theta_s(t)\rangle) - (\theta_g(t) - E\langle\theta_g(t)\rangle))^2\rangle} \quad (3)$$

$$R = \frac{E\langle(\theta_s(t) - E\langle\theta_s(t)\rangle) \cdot (\theta_g(t) - E\langle\theta_g(t)\rangle)\rangle}{\sigma_s \cdot \sigma_g} \quad (4)$$

Where $E\langle \cdot \rangle$ is the representation of the linear averaging operator, t is the time of observations, $\theta_s(t)$ represents the satellite SM products at time t , $\theta_g(t)$ represents the true observation based on the averaged ground measurements at time t . In addition, σ_s and σ_g represent the standard deviation of satellite SM measurements and ground observations, respectively.

The Taylor diagram (Taylor 2001) has been used to provide a brief statistical summary of how closely the datasets match observations in this paper, since the diagram can demonstrate the performance of various products in a single diagram in terms of the correlation coefficient, centered RMSE (i.e., ubRMSE), and standard deviation.

Results

In this section, we analyzed the performance of seven soil moisture products in each network respectively. For each network, First, we analyze the temporal variation of in-situ SM and satellite SM products according to the time of satellite ascending and descending during the entire period, which can declare the performance of SM products in season and year. Precipitation information was added to each time series as auxiliary information as shown in Figs. 2, 5

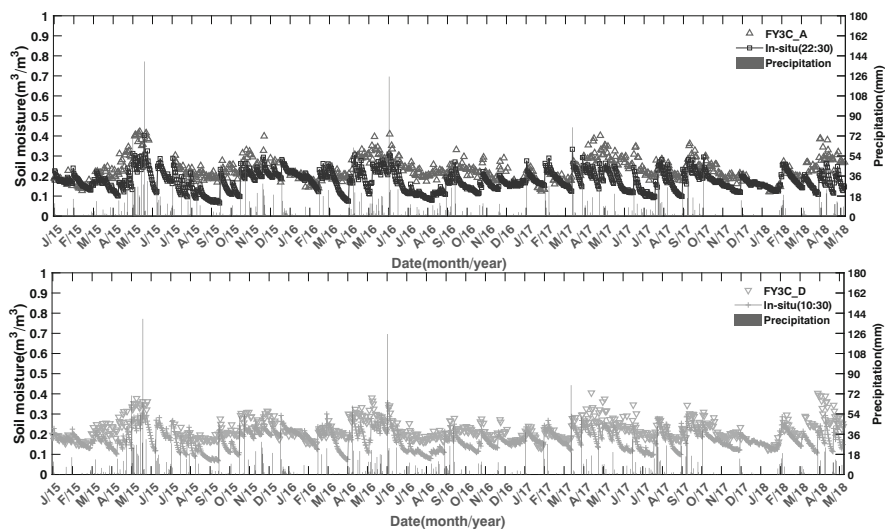
Fig. 2 Time series variation over the LW network: **a** FY3C_A and FY3C_D SM products time series variation over the LW network, **b** FY3B_A, FY3B_D, JAXA AMSR2_A, JAXA AMSR2_D, LPRM AMSR2_A, LPRM AMSR2_D, LPDR_A and LPDR_D SM products time series variation over the LW network, **c** SMOS_A, SMOS_D, SMAP_A and SMAP_D and ESA CCI SM SM products time series variation over the LW network

and 8, respectively. In order to further explore the performance of satellite products, we investigated the scatter plots of station-averaged and satellite SM at am and pm, shown in Figs. 3, 6 and 9. And four error metrics (R, Bias, RMSE, ubRMSE) were used to evaluate the specific performance of satellite ascending orbit and descending orbit products, respectively, summarized in Tables 1 to 3. Taylor diagram can more clearly compare the performance of seven SM products, shown in Figs. 4, 7 and 10.

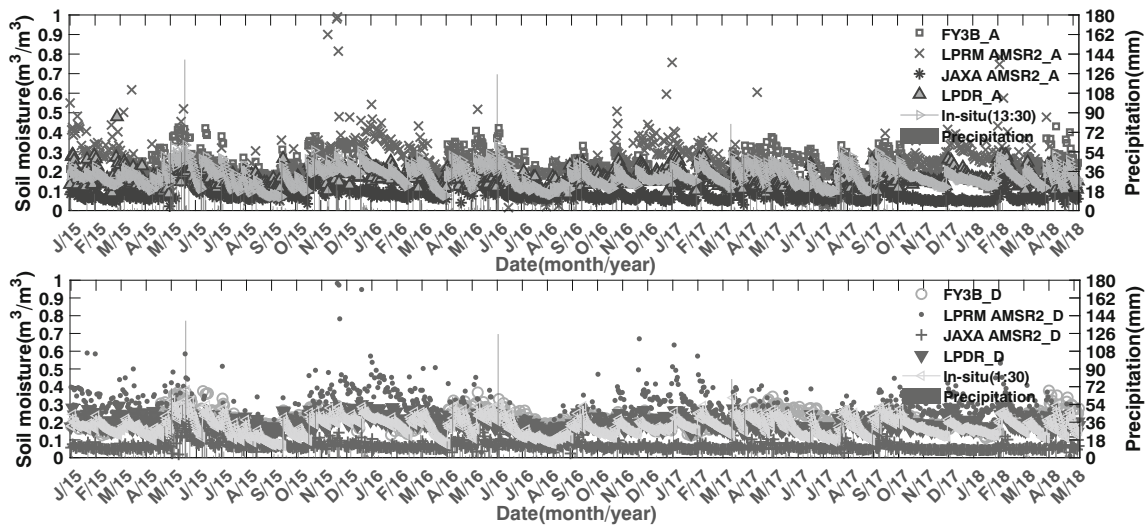
Figures 2, 5, 8 and 3, 6, 9 represent the time series and the scatterplot of the station-averaged SM and eight SM products for both ascending and descending orbit data during 1 Jan 2015 to 1 May 2018. The red triangle represents FY3C_A SM products, The green inverted triangle represents FY3C_D SM products, the red diamond represents SMOS_A SM products, the green five-pointed star represents SMOS_D SM products, the cyan star represents JAXA AMSR2_A SM products, the brown plus sign represents JAXA AMSR2_D SM product, the red left triangle star represents SMAP_A SM product, the blue hexagram represents SMAP_D SM product, the brown plus sign represents LPRM AMSR2_A SM product, the brown cross represents LPRM AMSR2_D SM product, The green solid triangle represents LPDR_A SM products, The red inverted solid triangle represents LPDR_D SM products The different lines with the symbol represent in-situ SM. Considering that LPRM retrieval values are extreme values that will affect the evaluation results; therefore, the maximum LPRM AMSR2 retrievals ($0.99 \text{ m}^3 \text{ m}^{-3}$) were deleted in the following section.

LW network

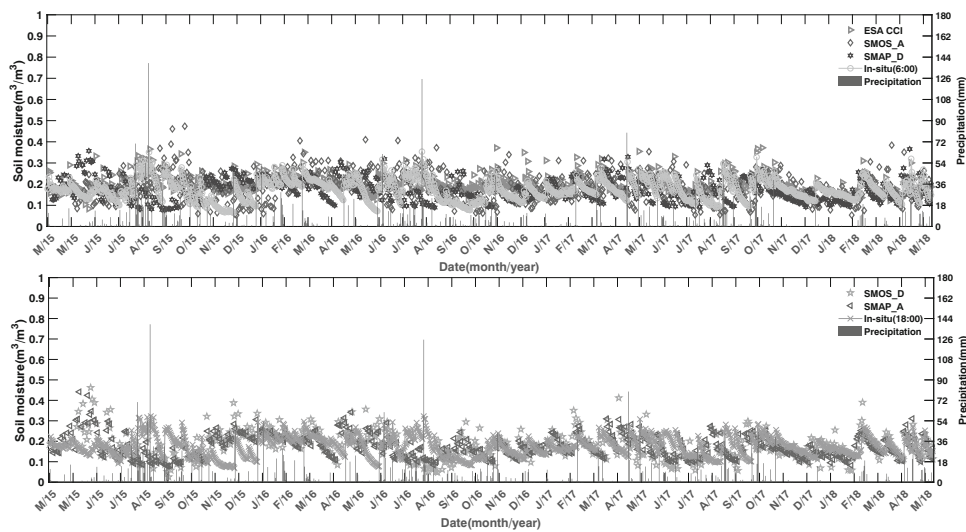
As shown in Fig. 2, the rainfall in the LW network area changes significantly throughout the year, and most of the rainfall is concentrated in the monsoon season (May to October each year). It can also be seen that the in-situ SM has a good response to precipitation and there is a good agreement between them. The site-averaged SM ranges from 0.06 to $0.38 \text{ m}^3 \text{ m}^{-3}$ in the evaluation domain. The eight SM products are sensitive to the change of precipitation, which can better reflect the change trend of precipitation with time. Overall, the eight products can well reflect the SM dynamic range during the entire period but show different seasonal amplitudes. The



(a)



(b)



(c)

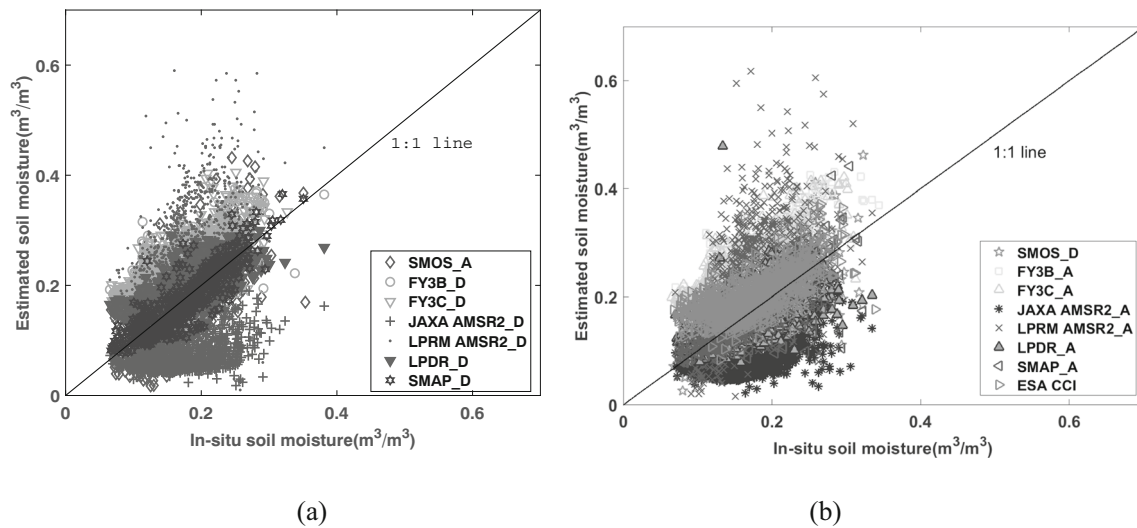


Fig. 3 Scatterplots of daily satellite soil moisture products with the ground measurements for the morning and afternoon orbits in the evaluation domain over the LW Network: **a** morning orbit and **b** afternoon orbit

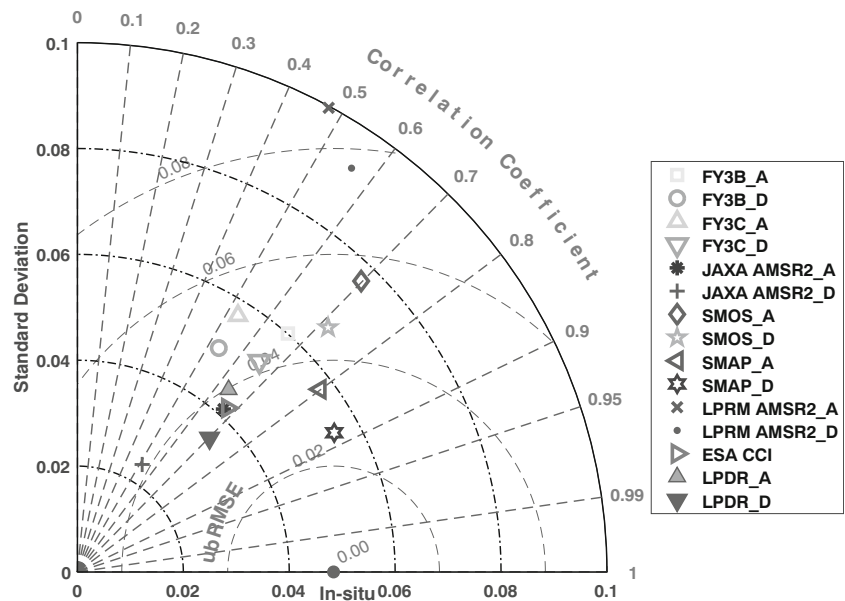
SMAP_D SM product performs very well in the LW network region with the lowest RMSE and ubRMSE values as well as the highest R value. It can be seen from the Fig.2(c) that it is highly consistent with the measured SM change trend during the entire period. The correlation coefficient of the SMOS_A, SMOS_D, SMAP_A, SMAP_D SM products were 0.698,0.716,0.799 and 0.879 respectively, which are also higher than that of FY3B, FY3C, JAXA AMSR2 and

LPRM AMSR2. It was observed that SMOS and SMAP SM products could capture the temporal variations of near-surface soil moisture better than FY3B, FY3C, JAXA AMSR2 and LPRM AMSR2 SM products. This was consistent with the general expectation that the L-band has a deeper depth of emission layer and less susceptible to the influences of vegetation and atmosphere compared to higher frequencies, such as the C-band and the X-band. The JAXA AMSR2_A and JAXA AMSR2_D SM products underestimated SM most of the time, with a dry bias of $-0.088 \text{ m}^3 \text{ m}^{-3}$ and $-0.109 \text{ m}^3 \text{ m}^{-3}$, respectively. This was generally in accordance with previous studies, JAXA AMSR2 usually underestimates in-situ measurements (Cui et al. 2017). It was worth noting that although JAXA AMSR2 had a higher RMSE, lower ubRMSE. One of the possible reasons is that the SM change trend of JAXA AMSR2 is small. According to formula 3, the two variables are subtracted and become smaller. The LPRM AMSR2_A and LPRM AMSR2_D SM products evidently overestimated the SM most of the time, with a wet bias of $0.056 \text{ m}^3 \text{ m}^{-3}$ and $0.100 \text{ m}^3 \text{ m}^{-3}$ respectively, as shown in Fig. 4 and Table 1. The LPDR_A and LPDR_D SM products were superior to the other two AMSR2 SM products, with a higher correlation coefficient and smaller RMSE values. And LPDR_D SM products were better than LPDR_A SM products. The ESA CCI SM product had a lower RMSE than FY3B, FY3C, JAXA AMSR2 and LPRM AMSR2 SM products. FY3B and FY3C both of ascending and descending orbit products overestimate SM most of the time, with a damp bias of $0.061 \text{ m}^3 \text{ m}^{-3}$, $0.053 \text{ m}^3 \text{ m}^{-3}$, $0.064 \text{ m}^3 \text{ m}^{-3}$ and $0.054 \text{ m}^3 \text{ m}^{-3}$, respectively, and the fluctuation range of FY3B and FY3C were larger than that of measured SM. FY3B_A and FY3C_D products are comparable in terms of correlation (0.662 and 0.654, respectively). Additionally, the

Table 1 Error metrics of soil moisture for LW network. RMSE (root mean square error), Bias (mean bias) and ubRMSE (unbiased RMSE) are both in $\text{m}^3 \text{ m}^{-3}$, R is the correlation coefficient, N is the number of samples. Bold data in the table represent the best results concerning each error metric

| Products | R | Bias | RMSE | ubRMSE | N |
|--------------|--------------|--------------|--------------|--------------|-----|
| FY3B_A | 0.662 | 0.061 | 0.076 | 0.046 | 743 |
| FY3B_D | 0.534 | 0.053 | 0.072 | 0.049 | 642 |
| FY3C_A | 0.531 | 0.064 | 0.082 | 0.052 | 667 |
| FY3C_D | 0.654 | 0.054 | 0.068 | 0.042 | 682 |
| JAXA AMSR2_A | 0.667 | -0.088 | 0.095 | 0.037 | 998 |
| JAXA AMSR2_D | 0.516 | -0.109 | 0.117 | 0.043 | 959 |
| SMOS_A | 0.698 | -0.023 | 0.059 | 0.055 | 591 |
| SMOS_D | 0.716 | 0.000 | 0.046 | 0.046 | 593 |
| SMAP_A | 0.799 | -0.001 | 0.035 | 0.035 | 566 |
| SMAP_D | 0.879 | -0.004 | 0.027 | 0.026 | 566 |
| LPRM AMSR2_A | 0.476 | 0.056 | 0.104 | 0.088 | 857 |
| LPRM AMSR2_D | 0.561 | 0.100 | 0.126 | 0.076 | 884 |
| ESA CCI | 0.675 | 0.027 | 0.046 | 0.037 | 974 |
| LPDR_A | 0.638 | -0.010 | 0.041 | 0.039 | 826 |
| LPDR_D | 0.702 | 0.020 | 0.040 | 0.034 | 823 |

Fig. 4 Taylor diagrams of LW network

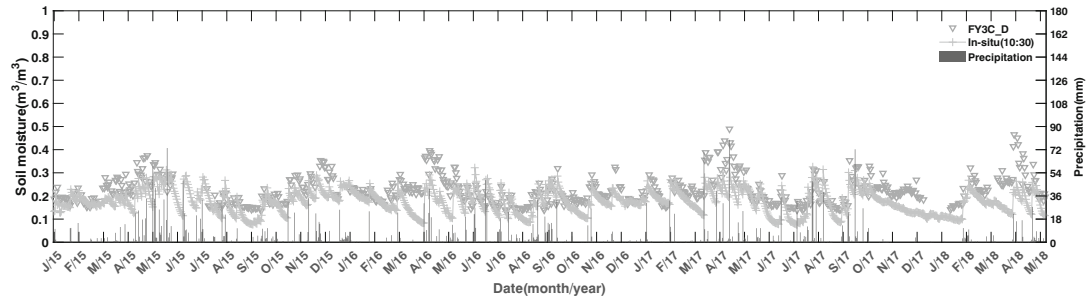
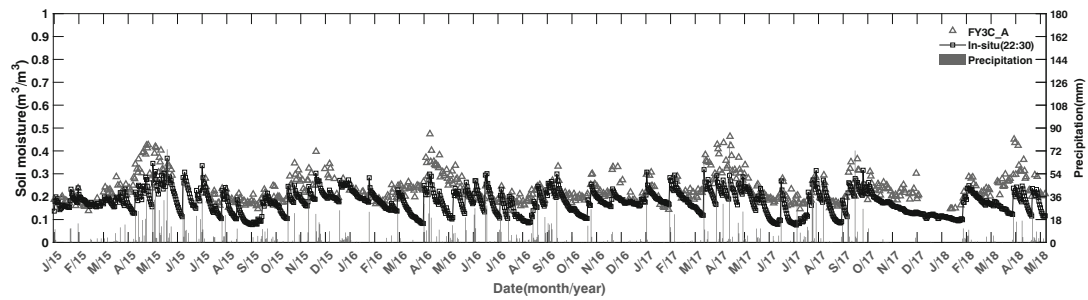


Taylor diagram was used to provide a comprehensive view of how closely the satellite products matched the ground measurements. Taylor chart shows more clearly the relationship between satellite products and measured SM. As illustrated in Fig. 4, the variability of SMAP_A and SMAP_D SM products were very closed in-situ soil moisture, whereas LPRM AMSR2 SM products were more variable than in-situ SM, and JAXA AMSR2 showed a lower variability than the in-situ observations.

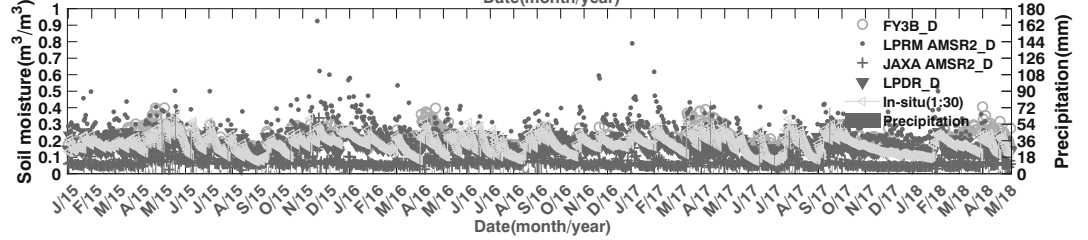
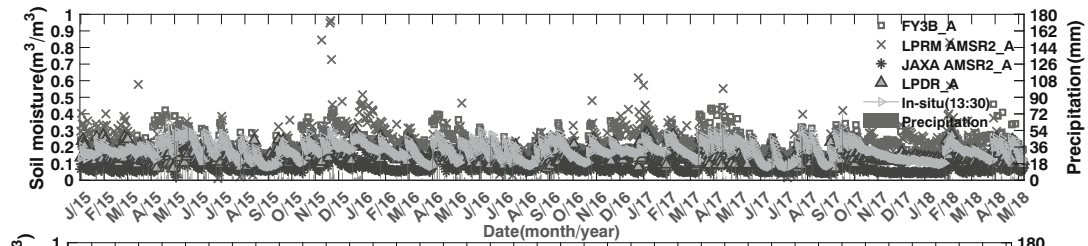
FC network

As shown in Fig. 5, precipitation had a significant effect on measured SM and satellite SM. Both the in-situ SM and satellite SM can respond well to precipitation. When the precipitation increases, the corresponding measured SM and satellite SM increase. It was observed that the FY3B_A, FY3B_D, FY3C_A and FY3C_D still overestimated SM over FC network, with a wet bias (0.091 m³ m⁻³, 0.079 m³ m⁻³, 0.093 m³ m⁻³, 0.103 m³ m⁻³ respectively) similar to that found over the LW network. When there is more precipitation, the overestimation is more obvious, as shown in Fig.5. FY3B_A and FY3C_D SM products were superior to FY3B_D and FY3C_A SM products respectively, with a high correlation coefficient of 0.714 and 0.677, as shown in Fig. 6 and Table 2. JAXA AMSR2_A and JAXA AMSR2_D products still underestimate soil moisture, with a dry bias (-0.093 m³ m⁻³, -0.110 m³ m⁻³, respectively) similar to discovered in the LW network. And JAXA AMSR2_A SM product surpassed JAXA AMSR2_D, which had the lowest ubRMSE of 0.036 m³ m⁻³. The LPRM AMSR2_A

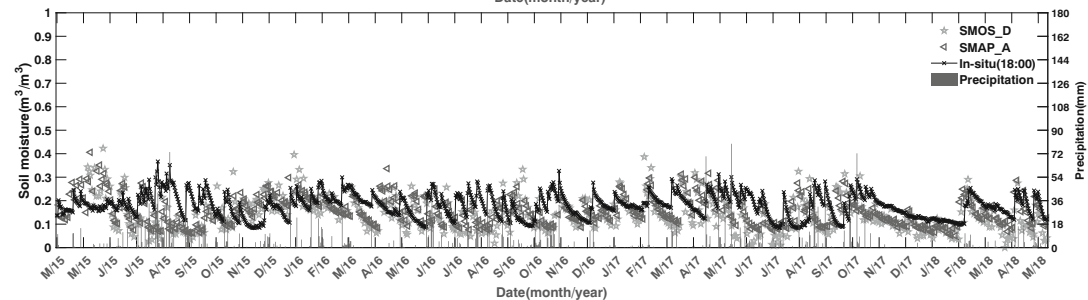
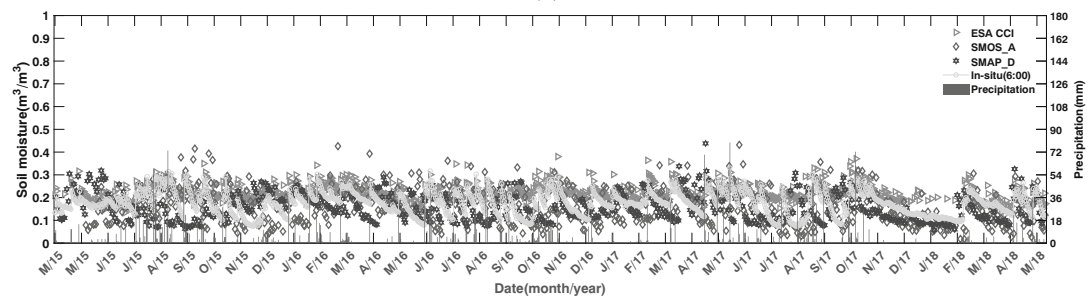
and LPRM AMSR2_D SM products still evidently overestimated the SM most of the time, with a wet bias of 0.037m³ m⁻³ and 0.072 m³ m⁻³ respectively, as shown in Fig. 5 and Table 2. In terms of X-band comparison, FY3B_D SM product had a lower RMSE than JAXA AMSR2 and LPRM AMSR2 SM products. The LPDR_A and LPDR_D SM products underestimated ground measurements, with a dry bias (-0.031 m³ m⁻³, -0.005 m³ m⁻³, respectively). The LPDR_D SM products outperformed LPDR_A SM products, with a small ubRMSE of 0.034 m³ m⁻³ and a high correlation coefficient of 0.733. The LPDR SM products performed well than other AMSR2 SM products in the FC network. The LPDR_A LPDR_D SM product had the highest correlation coefficient among all the X-band satellite SM products. SMOS products both of ascending orbit and descending orbit had a higher correlation coefficient (0.733 and 0.724, respectively) than X-band satellite SM products, which suggests that SMOS well captures the change trend of observations in the FC network. SMOS_A SM product outperformed the SMOS_D SM product and SMOS_A and SMOS_D had a dry bias of 0.024 m³ m⁻³ and 0.037 m³ m⁻³, which was contrary to the results found in the LW network. And SMOS SM products both of ascending orbit and descending orbit had noisy and unstable results in both of the LW network and the FC network. The SMAP_D SM product performs very well in the FC network region with the lowest Bias, RMSE and ubRMSE as well as the highest R value. SMAP SM products outperformed the SMOS SM products and other X-band satellite SM products. In addition, as shown in Fig. 7, it can be seen that the time variation of the



(a)



(b)



(c)

Fig. 5 Time series variation over the FC network: **a** FY3C_A and FY3C_D SM products time series variation over the FC network, **b** FY3B_A, FY3B_D, JAXA AMSR2_A, JAXA AMSR2_D, LPRM AMSR2_A, LPRM AMSR2_D, LPDR_A and LPDR_D SM products time series variation over the FC network, **c** SMOS_A, SMOS_D, SMAP_A and SMAP_D and ESA CCI SM products time series variation over the FC network

SMAP_D product was in accordance with that of in-situ SM, whereas JAXA AMSR2_D still had a lower variability than the in-situ observations.

Yanco network

In the Yanco network, the in-situ SM was overestimated by the FY3B_A, FY3B_D, FY3C_A, FY3C_D, LPRM AMSR2_A and LPRM AMSR2_D SM products with wet bias ($0.091 \text{ m}^3 \text{ m}^{-3}$, $0.079 \text{ m}^3 \text{ m}^{-3}$, $0.093 \text{ m}^3 \text{ m}^{-3}$, $0.103 \text{ m}^3 \text{ m}^{-3}$, $0.007 \text{ m}^3 \text{ m}^{-3}$ and $0.043 \text{ m}^3 \text{ m}^{-3}$, respectively), which is similar to the results in both of LW network and FC network. Overestimation is more pronounced during continuous rainfall, as shown in Fig. 8. FY3B_A SM product was superior to FY3B_D SM product, which had a higher correlation coefficient of 0.694 and a lower ubRMSE $0.104 \text{ m}^3 \text{ m}^{-3}$. As shown in the Fig. 8, FY3B and FY3C SM products had a noisy performances of capturing temporal variations. Moreover, in Fig. 8, the soil moisture value of FY3B and FY3C SM products were almost $0.5 \text{ m}^3 \text{ m}^{-3}$ occasionally. The reason was that the time period was continuous precipitation making the surface SM saturated. However, the saturated SM used in the FY3B and FY3C retrieval algorithm is $0.5 \text{ m}^3 \text{ m}^{-3}$, not very consistent with the in-suit measurements. JAXA AMSR2_A and JAXA AMSR2_D SM products still

Table 2 Error metrics of soil moisture for FC network. RMSE (root mean square error), Bias (mean bias) and ubRMSE (unbiased RMSE) are both in $\text{m}^3 \text{ m}^{-3}$, R is the correlation coefficient, N is the number of samples. Bold data in the table represent the best results concerning each error metric

| Products | R | Bias | RMSE | ubRMSE | N |
|--------------|--------------|---------------|--------------|--------------|------|
| FY3B_A | 0.714 | 0.053 | 0.070 | 0.046 | 740 |
| FY3B_D | 0.604 | 0.046 | 0.065 | 0.046 | 655 |
| FY3C_A | 0.597 | 0.060 | 0.079 | 0.051 | 645 |
| FY3C_D | 0.677 | 0.048 | 0.066 | 0.046 | 687 |
| JAXA AMSR2_A | 0.713 | -0.093 | 0.100 | 0.036 | 957 |
| JAXA AMSR2_D | 0.562 | -0.110 | 0.117 | 0.042 | 935 |
| SMOS_A | 0.796 | -0.024 | 0.053 | 0.047 | 598 |
| SMOS_D | 0.764 | -0.037 | 0.060 | 0.046 | 563 |
| SMAP_A | 0.795 | -0.022 | 0.044 | 0.038 | 564 |
| SMAP_D | 0.898 | -0.020 | 0.034 | 0.027 | 566 |
| LPRM AMSR2_A | 0.512 | 0.037 | 0.086 | 0.077 | 918 |
| LPRM AMSR2_D | 0.614 | 0.072 | 0.098 | 0.066 | 902 |
| ESA CCI | 0.644 | 0.042 | 0.057 | 0.038 | 1082 |
| LPDR_A | 0.674 | -0.031 | 0.049 | 0.039 | 813 |
| LPDR_D | 0.733 | -0.005 | 0.035 | 0.034 | 757 |

underestimated in-situ SM, with a dry bias ($-0.065 \text{ m}^3 \text{ m}^{-3}$, $-0.081 \text{ m}^3 \text{ m}^{-3}$ respectively) in line with that found in the LW network and FC network. The LPDR_A and LPDR_D SM products underestimated compared to the in-situ measured SM, with a dry bias ($-0.059 \text{ m}^3 \text{ m}^{-3}$, $-0.038 \text{ m}^3 \text{ m}^{-3}$ respectively) in line with that found in the FC network. The LPDR_A had a higher correlation coefficient than the LPDR_D, which was different from the result of in the FC and LW network. And From the Table 3, it can be seen that

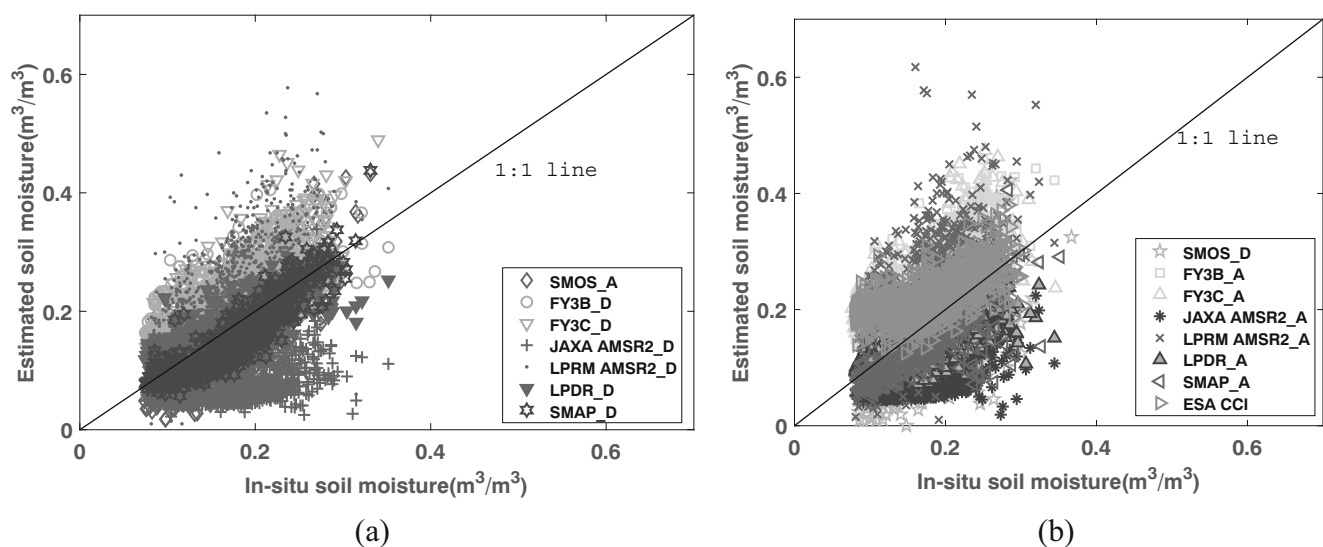


Fig. 6 Scatterplots of daily satellite soil moisture products with the ground measurements morning orbits afternoon orbits in the evaluation domain over the FC network: **a** morning orbit and **b** afternoon orbit

SMOS_A and SMOS_D SM products are all overestimated compared to in-situ SM, with a wet bias of $0.024 \text{ m}^3 \text{ m}^{-3}$ and $0.019 \text{ m}^3 \text{ m}^{-3}$ respectively, but their correlation with ground measurements were higher than other satellite products. The SMOS_A SM product was superior to SMOS_D product, which had the great correlation coefficient of 0.852 and the lowest ubRMSE of $0.064 \text{ m}^3 \text{ m}^{-3}$. From the Fig. 8(c), we found that SMOS SM products occasionally show abnormally high values. The possible reason may be SMOS SM product affected by RFI in this network. SMAP_A SM product outperformed the SMAP_D SM product, which was contrary to the results found in the LW network and FC network. The ESA CCI SM product showed good agreement with the in-situ SM in the Yanco network, with an ubRMSE value of $0.044 \text{ m}^3 \text{ m}^{-3}$ and a RMSE value of $0.049 \text{ m}^3 \text{ m}^{-3}$, which was smaller than SMOS, SMAP, LPRM AMSR2 and JAXA AMSR2 SM products. This was in agreement with the results reported in (Cui et al. 2018), revealing the effectiveness of merging active and passive SM products to improve the accuracy of a single satellite SM product (Fig. 9). Besides, it was found that the ESA CCI SM product had the highest number of valid values than other satellite SM products. From Fig. 10, it can be seen that the variability of LPRM AMSR2_A was very close to that of the in-situ SM, and ESA CCI SM product showed a lower variability than the ground measurements.

Discussion

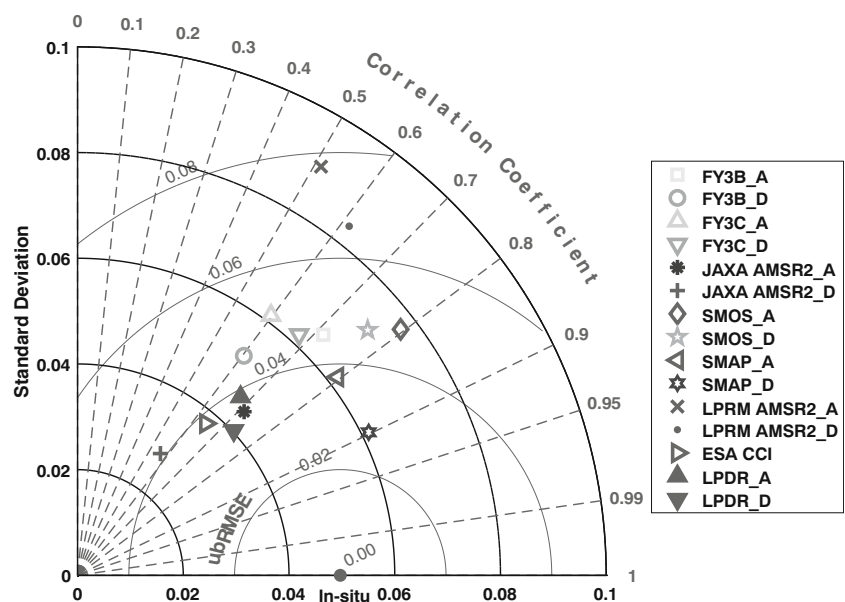
In this study, we evaluated the performance of eight SM products using measured soil moisture from three observation networks in two different regions. Long time series and statistical

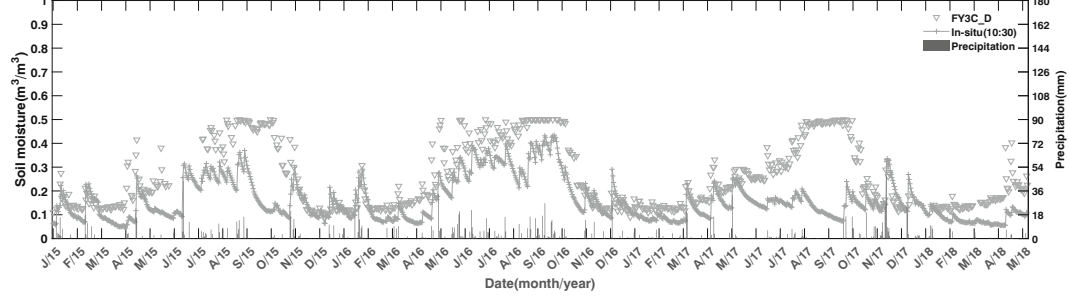
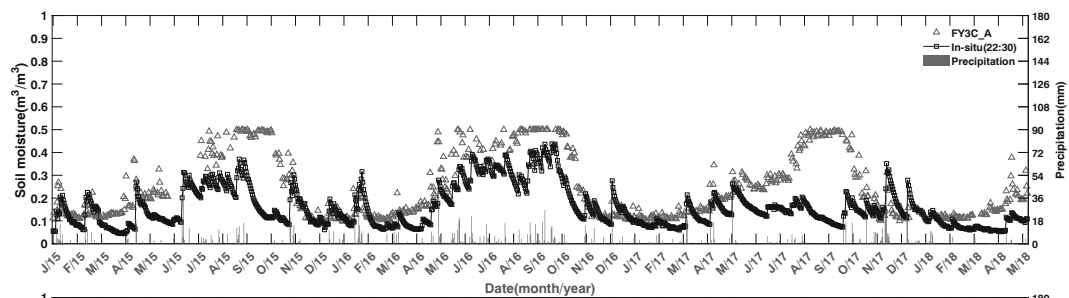
Fig. 8 Time series variation over the Yanco network: **a** FY3C_A and FY3C_D SM products time series variation over the Yanco network, **b** FY3B_A, FY3B_D, JAXA AMSR2_A, JAXA AMSR2_D, LPRM AMSR2_A, LPRM AMSR2_D, LPDR_A and LPDR_D SM products time series variation over the Yanco network, **c** SMOS_A, SMOS_D, SMAP_A and SMAP_D and ESA CCI SM products time series variation over the Yanco network

indicators showed that FY3B and FY3C obvious overestimate in-situ soil moisture in three soil moisture networks in two different regions. On the contrary, JAXA AMSR2 products obviously underestimated the ground soil moisture in all networks. The LPDR SM products performed well than the other AMSR2 products in the LW and FC networks. The SMOS and SMAP SM products surpassed FY3B, FY3C, JAXA AMSR2 and LPRM AMSR2 SM products, which had a higher correlation coefficient than other satellite products. Following, we discussed the factors that contribute to the different performance of satellite products.

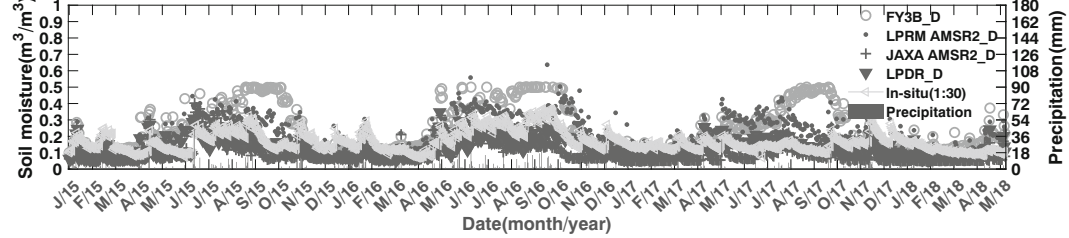
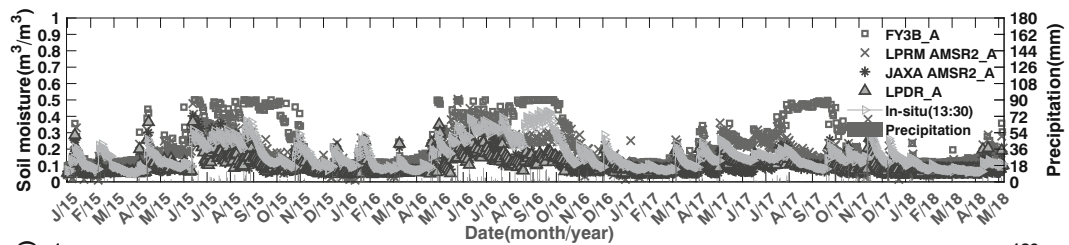
First, there is a large scale mismatch between in-situ and satellite-based measurements. The monitoring station provides soil moisture measurements at point locations, typically measured in centimeters, while microwave sensors on the satellite measure the average soil moisture within a satellite footprint, such as the FY3B, FY3C and SMOS satellite pixel scales of approximately 25 km, and the spatial heterogeneity of surface soil moisture will cause spatial average soil moisture in satellite footprints to differ from point-based field measurements. Second, sensor depth mismatch between on-site soil moisture and satellite observations may also create uncertainty in the assessment results. FY3B, FY3C, LPRM AMSR2, JAXA AMSR2 and LPDR use X-band to retrieve soil moisture, the X-band penetration depth to the surface is 0–

Fig. 7 Taylor diagrams of FC network

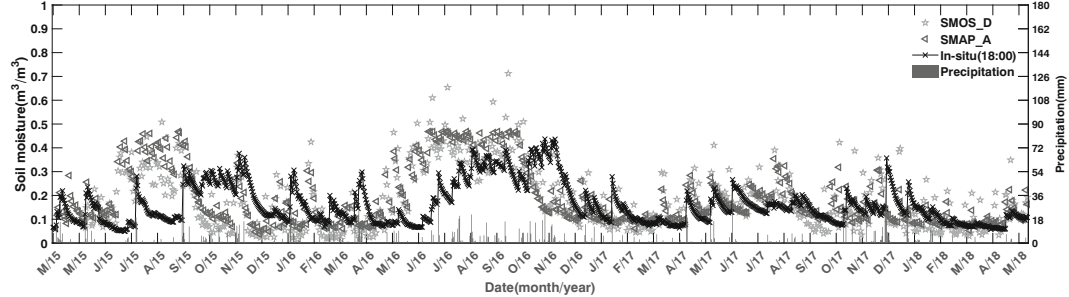
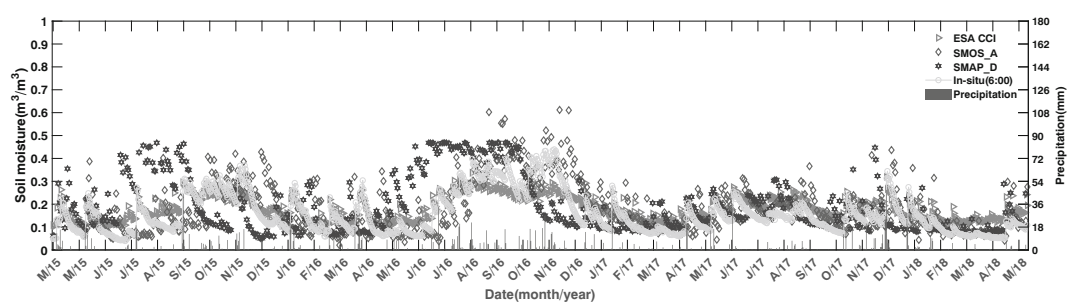




(a)



(b)



(c)

Table 3 Error metrics of soil moisture for Yanco network. RMSE (root mean square error), Bias (mean bias) and ubRMSE (unbiased RMSE) are both in $\text{m}^3 \text{m}^{-3}$, R is the correlation coefficient, N is the number of samples. Bold data in the table represent the best results concerning each error metric

| Products | R | Bias | RMSE | ubRMSE | N |
|--------------|--------------|---------------|--------------|--------------|------|
| FY3B_A | 0.694 | 0.091 | 0.138 | 0.104 | 807 |
| FY3B_D | 0.428 | 0.079 | 0.145 | 0.122 | 743 |
| FY3C_A | 0.656 | 0.093 | 0.140 | 0.105 | 707 |
| FY3C_D | 0.636 | 0.103 | 0.148 | 0.106 | 682 |
| JAXA AMSR2_A | 0.728 | -0.065 | 0.087 | 0.058 | 940 |
| JAXA AMSR2_D | 0.522 | -0.081 | 0.099 | 0.056 | 946 |
| SMOS_A | 0.864 | 0.024 | 0.064 | 0.060 | 616 |
| SMOS_D | 0.806 | 0.019 | 0.084 | 0.082 | 610 |
| SMAP_A | 0.934 | 0.027 | 0.058 | 0.052 | 567 |
| SMAP_D | 0.868 | 0.032 | 0.070 | 0.062 | 569 |
| LPRM AMSR2_A | 0.786 | 0.007 | 0.059 | 0.059 | 921 |
| LPRM AMSR2_D | 0.553 | 0.043 | 0.100 | 0.090 | 920 |
| ESA CCI | 0.865 | 0.020 | 0.049 | 0.044 | 1027 |
| LPDR_A | 0.719 | -0.059 | 0.084 | 0.060 | 834 |
| LPDR_D | 0.621 | -0.038 | 0.064 | 0.051 | 808 |

1 cm. However, SMOS products use L-band to invert soil moisture, which typically up to 5 cm depth and the sensor to obtain the measured soil moisture is deployed 5 cm below the soil surface. From three networks results, we could find SMOS product had a high correlation coefficient than other X-band products. Although the FY3B and FY3C satellite sensors are the same, they have different accuracy. One important reason is that FY3B and FY3C have different ascending and descending time. FY3B's ascending time is about 13:30 in the

afternoon while FY3C's ascending time is about 22:30, which lead to accuracy difference among the FY sensors. The ascending and descending time of FY3B. Finally, the errors from retrieval algorithms and their inputs play an important role in the performance of soil moisture products. Because the LPDR was generated using similar calibrated, multifrequency brightness temperature (T_b) retrievals from the AMSR-E and the AMSR2, they were not listed in Table 4. Frequency, surface temperature, vegetation correction, and roughness are the main factors affecting the passive microwave remote sensing of soil moisture (Jackson 1993). Therefore, the different model parameters in the five algorithms, i.e., the brightness temperature, physical surface temperature, surface roughness and vegetation dynamics, are summarized in Table 4.

Frequency: The JAXA AMSR2, LPRM AMSR2, FY3B, FY3C and LPDR SM products provide SM retrievals from the Earth's surface using the X band observations. The SMOS and SMAP are equipped with L-band sensors designed for SM retrieval. From the results in fourth section, L-band SM products have better accuracy than X-band.

Vegetation optical depth (τ): The JAXA is essentially a look-up table method with a linear relationship between τ and VWC (Jackson and Schmugge 1991). The LPRM optical depth is expressed in terms of mixed dielectric constant, the incidence angle, and the microwave polarization difference index (MPDI) (Meesters et al. 2005). The SMOS assumes that the nadir estimate of the overall optical depth is independent from the incidence angle (θ) and polarization (p) and the function (θ , p) (Kerr et al. 2012).

Surface roughness: FY3B and FY3C is based on the Qp model and eliminates the effect of roughness (Shi et al. 2005).

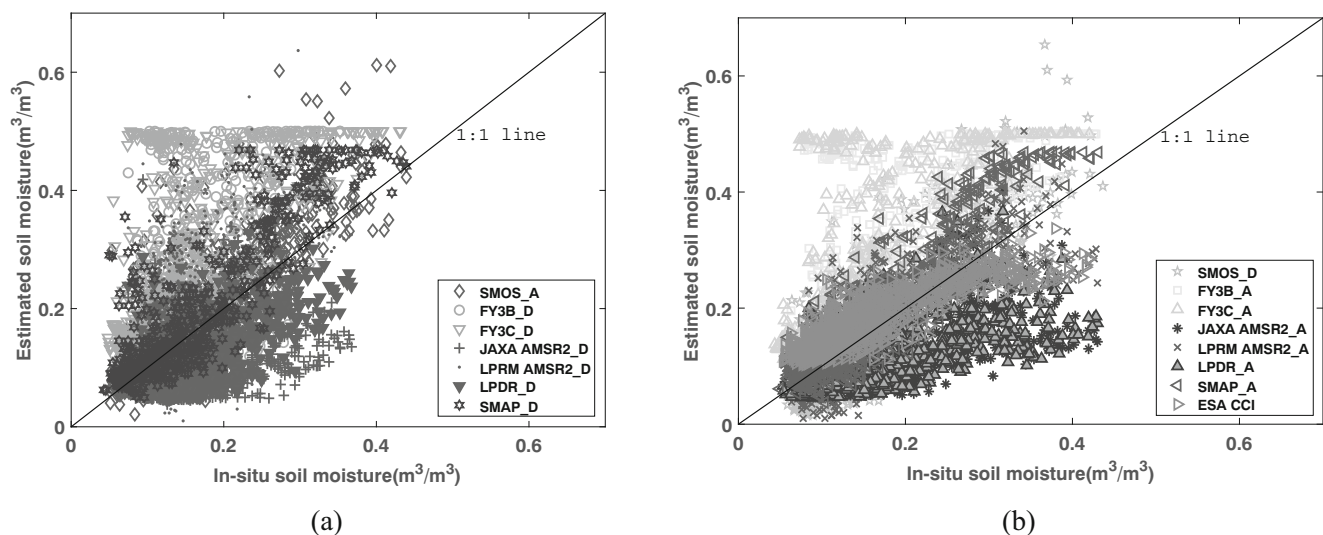
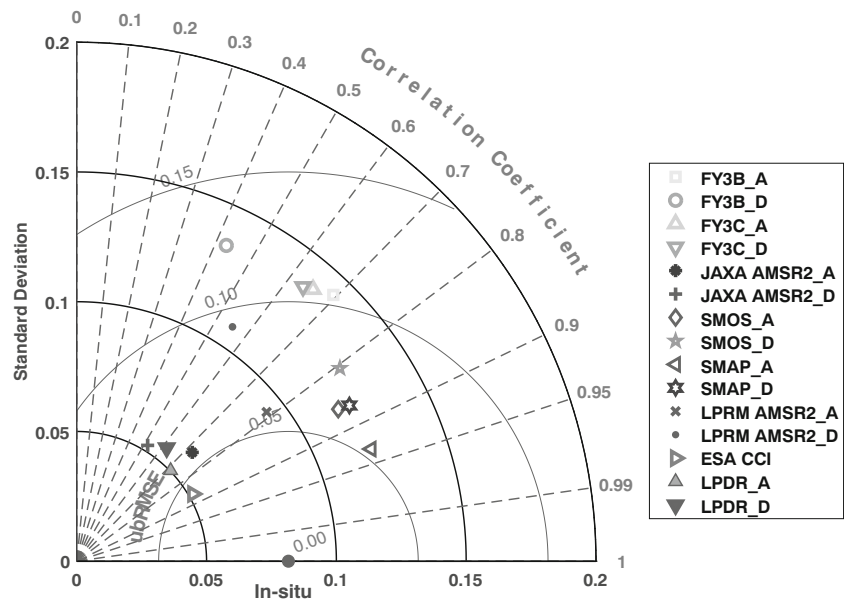


Fig. 9 Scatterplots of daily satellite soil moisture products with the ground measurements for the morning and afternoon orbits in the evaluation domain over the Yanco network: **a** morning orbit and **b** afternoon orbit

Fig. 10 Taylor diagrams of Yanco network



The surface roughness in the JAXA and LPRM algorithms is assumed to be constant (Wang and Choudhury 1981; Njoku and Li 1999). From the results in fourth section, FY3B and FY3C had lower RMSE values than JAXA AMSR2 and LPRM AMSR2 in the FC network. The constant assumption of the surface roughness will inevitably bring errors to the satellite SM retrievals.

Conclusions

In this study, we evaluated seven currently frequently-used soil moisture (FY3B_A, FY3B_D, FY3C_A, FY3C_D, JAXA AMSR2_A, JAXA AMSR2_D, LPRM AMSR2_A, LPRM AMSR2_D, LPDR_A, LPDR_D, SMOS_A,

SMOS_D, SMAP_A and SMAP_D) in three dense networks over two different regions.

Compared to the station-averaged measurements, the FY3B_A, FY3B_D, FY3C_A, FY3C_D, LPRM AMSR2_A and LPRM AMSR2_D SM products overestimated soil moisture in LW, FC and Yanco networks. It is more severe overestimation especially in Yanco network. JAXA AMSR2_A and JAXA AMSR2_D had an obvious underestimate in three networks. The LPDR SM products SMOS_A and SMOS_D had a higher time series correlation coefficients than X-band products in three networks, but SMOS products had a noisy and unstable results with ground soil moisture. SMAP_A and SMAP_D SM products had the most highest values of R than other products in three networks, SMAP_D SM product outperformed SMAP_A SM product in the LW and FC

Table 4 summary of the six soil moisture products retrieval algorithm

| Parameters | FY3B and FY3C | JAXA AMSR2 | LPRM AMSR2 | SMOS | SMAP |
|-----------------------|----------------------------|--|--|--|--|
| Frequency (GHz) | 10.65, 18.7, 36.5 | 10.65, 36.5 | 6.93, 10.65, 36.5 | 1.4 | 1.41 |
| Soil and vegetation | – | $T_S = T_C = 293$ K | $T_S = T_C$ linearly | European Centre for Medium-Range Weather Forecasts (ECMWF) products | $T_S = T_C$ GEOS-5 products |
| Physical temperatures | related with TB (37 GHz_V) | – | related with TB (37 GHz_V) | – | – |
| Vegetation | $\tau_C = b \cdot VWC$ | $\tau_C = b \cdot VWC$ | $\tau_C = f(MPDI, k, u, \omega)$ | $\tau_C = \tau_{NAD} \cdot f(\theta, p)$ | $\tau_C = b \cdot VWC$ VWC = $f(NDVI)$ Nonlinear VWC |
| Surface roughness | Qp model Shi et al. 2005 | Constants Q, H Wang and Choudhury 1981 | Constants Q, H Wang and Choudhury 1981 | Escorihuela et al. 2007 combine with Wang and Choudhury 1981 Q/H model | Q/H model Choudhury et al. 1979 |

T_S : soil surface temperature; T_C : vegetation canopy temperature; Q: polarization mixing ratio; H: roughness parameters;; TB: brightness temperature; τ_C : optical depth; τ_{NAD} : nadir estimate of overall optical depth; p: Polarization; ω : single scattering albedo; b: Vegetation parameter; VWC: vegetation water content; f_c : fractional vegetation coverage; MPDI: microwave polarization difference index

network. ESA CCI SM products had the lowest values of RMSE and ubRMSE in the Yanco network. Overall, SMAP products had a better performance than other products in three networks.

Acknowledgements This work was funded by the National Natural Science Foundation of China (41501409), Natural Science Foundation of Shandong Province (ZR2015DL003). We are indebted to the European Space Agency (ESA), and the Centre Aval de Traitement des Données SMOS (CATDS), Goddard Geoscience Data and Information Service (GES DISC), Japan Aerospace Exploration Agency (JAXA), National Snow and Ice Data Center (NSIDC), NASA MEaSUREs (Making Earth System Data Records for Use in Research Environments), University of Montana and CNSMC for providing the ESA CCI, SMOS, LPRM AMSR2, JAXA AMSR2, LPDR, SMAP, FY3B and FY3C soil moisture products, and the U.S. Department of Agriculture Agricultural Research Service and OzNet hydrological monitoring network for providing the in-situ data.

References

- Blonquist Jr JM, Jones SB, Robinson DA (2005) A time domain transmission sensor with TDR performance characteristics. *J Hydrol* 314(1–4):235–245
- Bolten JD, Crow WT, Zhan X et al (2009) Evaluating the utility of remotely sensed soil moisture retrievals for operational agricultural drought monitoring. *IEEE Journal of Selected Topics in Applied Earth Observations and Remote Sensing* 3(1):57–66
- Chan SK, Bindlish RE, O'Neill P et al (2016) Assessment of the smap passive soil moisture product. *IEEE Trans Geosci Remote Sens*:1–14
- Chen YY, Yang K, Qin J et al (2017) Evaluation of SMAP, SMOS, and AMSR2 soil moisture retrievals against observations from two networks on the Tibetan plateau. *J Geophys Res Atmos* 122(11):5780–5792
- Choudhury BJ, Schmugge TJ, Chang A et al (1979) Effect of surface roughness on the microwave emission from soils. *J Geophys Res Atmos* 84(C9):5699–5706
- Collow TW, Robock A, Basara JB et al (2012) Evaluation of SMOS retrievals of soil moisture over the Central United States with currently available in-situ observations. *J Geophys Res Atmos* 117(D9)
- Cui HZ, Jiang LM, Du JY et al (2017) Evaluation and analysis of AMSR-2, SMOS, and SMAP soil moisture products in the Genhe area of China. *J Geophys Res Atmos* 122(16):8650–8666
- Cui CY, Xu J, Zeng JY, Chen KS et al (2018) Soil moisture mapping from satellites: an Intercomparison of SMAP, SMOS, FY3B, AMSR2, and ESA CCI over two dense network regions at different spatial scales. *Remote Sens* 10(1):33
- Daly E, Porporato A (2005) A review of soil moisture dynamics: from rainfall infiltration to ecosystem response. *Environ Eng Sci* 22(1):9–24
- Dorigo W, Wagner W, Albergel C et al (2017) ESA CCI soil moisture for improved earth system understanding: state-of-the art and future directions. *Remote Sens Environ* 203:185–215
- Douville H, Chauvin F (2000) Relevance of soil moisture for seasonal climate predictions: a preliminary study. *Clim Dyn* 16(10–11):719–736
- Du JY, Kimball JS, Shi JC et al (2014) Inter-calibration of satellite passive microwave land observations from AMSR-E and AMSR2 using overlapping FY3B-MWRI sensor measurements. *Remote Sens* 6: 8594–8616
- Du JY, Kimball JS, Jones LA (2016) Passive microwave remote sensing of soil moisture based on dynamic vegetation scattering properties for AMSR-E. *IEEE Trans Geosci Remote Sens* 1–12
- Du JY, Kimball JS, Jones LA et al (2017) A global satellite environmental data record derived from AMSR-E and AMSR2 microwave earth observations. *Earth System Science Data* 9(2):791–808
- El Hajj M, Baghdadi N, Zribi M, Rodríguez-Fernández N, Wigneron JP, Al-Yaari A, Al Bitar A, Albergel C, Calvet JC (2018) Evaluation of SMOS, SMAP, ASCAT and Sentinel-1 soil moisture products at sites in southwestern France. *Remote Sens* 10(4):569
- Entekhabi D, Njoku EG, O'Neill PE et al (2010) The soil moisture active passive (SMAP) Mission. *Proc IEEE* 98(5):704–716
- Escorihuela MJ, Kerr YH, De Rosnay P et al (2007) A simple model of the bare soil microwave emission at L-band. *IEEE Trans Geosci Remote Sens* 45(7):1978–1987
- Holmes TRH, De Jeu RAM, Owe M et al (2009) Land surface temperature from ka band (37 GHz) passive microwave observations. *J Geophys Res* 114(D4):D04113
- Imaoka K, Maeda T, Kachi M et al (2012) Status of AMSR2 instrument on GCOM-W1. In earth observing missions and sensors: development, implementation, and characterization II. *Proc SPIE* 8528: 852815
- Jackson TJ (1993) III. Measuring surface soil moisture using passive microwave remote sensing. *Hydrol Process* 7(2):139–152
- Jackson TJ, Schmugge TJ (1991) Vegetation effects on the microwave emission of soils. *Remote Sens Environ* 36(3):203–212
- Jackson TJ, Cosh MH, Bindlish R et al (2010) Validation of advanced microwave scanning radiometer soil moisture products. *IEEE Trans Geosci Remote Sens* 48(12):4256–4272
- Jones LA, Ferguson CR, Kimball JS et al (2010) Satellite microwave remote sensing of daily land surface air temperature minima and maxima from AMSR-E. *IEEE Journal of Selected Topics In Applied Earth Observations And Remote Sensing* 3(1):111–123
- Kerr YH, Waldteufel P, Wigneron JP et al (2010) The SMOS Mission: new tool for monitoring key elements of the global water cycle. *Proc IEEE* 98(5):666–687
- Kerr YH, Waldteufel P, Richaume P et al (2012) The SMOS soil moisture retrieval algorithm. *IEEE Trans Geosci Remote Sens* 50(5):1384–1403
- Leroux DJ, Kerr YH, Al Bitar A et al (2013) Comparison between SMOS, VUA, ASCAT, and ECMWF soil moisture products over four watersheds in US. *IEEE Trans Geosci Remote Sens* 52(3): 1562–1571
- Li C, Lu H, Yang K et al (2018) The evaluation of SMAP enhanced soil moisture products using high-resolution model simulations and in-situ observations on the Tibetan plateau. *Remote Sens* 10(4):535
- Liu Q, Du JY, Shi JC et al (2013) Analysis of spatial distribution and multi-year trend of the remotely sensed soil moisture on the Tibetan plateau. *Sci. China* 56(12):2173–2185
- Liu YX, Yang YP, Yue XF (2018) Evaluation of satellite-based soil moisture products over four different continental in-situ measurements. *Remote Sens* 10(7):1161
- Meesters AGCA, Dejeu RAM, Owe M et al (2005) Analytical derivation of the vegetation optical depth from the microwave polarization difference index. *IEEE Geosci Remote Sens Lett* 2(2):121–123
- Mironov VL, Kosolapova LG, Fomin SV et al (2009) Physically and mineralogically based spectroscopic dielectric model for moist soils. *IEEE Trans Geosci Remote Sens* 47(7):2059–2070
- Njoku EG, Li L (1999) Retrieval of land surface parameters using passive microwave measurements at 6–18 GHz. *IEEE Trans Geosci Remote Sens* 37(1):79–93
- Njoku EG, Jackson TJ, Lakshmi V, Chan TK, Nghiem SV (2003) Soil moisture retrieval from AMSR-E. *IEEE Trans Geosci Remote Sens* 41(2):215–229

- Njoku EG, Ashcroft P, Chan TK et al (2005) Global survey and statistics of radio-frequency interference in amsr-e land observations. *IEEE Trans Geosci Remote Sens* 43(5):938–947
- Owe M, de Jeu R, Holmes T (2008) Multisensor historical climatology of satellite-derived global land surface moisture. *J Geophys Res* 113(F1). <https://doi.org/10.1029/2007JF000769>
- Parinussa RM, Wang G, Holmes TRH et al (2014) Global surface soil moisture from the microwave radiation imager on board the Fengyun-3B satellite. *Int J Remote Sens* 35(19):7007–7029
- Saini R, Wang G, Pal JS (2016) Role of soil moisture feedback in the development of extreme summer drought and flood in the United States. *J Hydrometeorol* 17(8):2191–2207
- Schmugge T, Gloersen P, Wilheit T et al (1974) Remote sensing of soil moisture with microwave radiometers. *J Geophys Res* 79(2):317–323
- Shi JC, Jiang LM, Zhang LX et al (2005) A parameterized multifrequency-polarization surface emission model. *IEEE Trans Geosci Remote Sens* 43(12):2831–2841
- Smith AB, Walker JP, Western AW, Young RI, Ellett KM, Pipunic RC, Grayson RB, Siriwardena L, Chiew FHS, Richter H (2012) The Murrumbidgee soil moisture monitoring network data set. *Water Resour Res* 48(7). <https://doi.org/10.1029/2012WR011976>
- Taylor KE (2001) Summarizing multiple aspects of model performance in a single diagram. *J Geophys Res Atmos* 106(D7):7183–7192
- Wagner W, Hahn S, Kidd R et al (2013) The ASCAT soil moisture product: a review of its specifications, validation results, and emerging applications. *Meteorol Z* 22(1):5–33
- Wang JR, Choudhury BJ (1981) Remote sensing of soil moisture content over bare field at 1.4 GHz frequency. *J Geophys Res* 86(C6)
- Wigneron JP, Kerr Y, Waldteufel P et al (2007) L-band microwave emission of the biosphere (L-MEB) model: description and calibration against experimental data sets over crop fields. *Remote Sens Environ* 107(4):639–655
- Yang J, Zhang P, Lu NM et al (2012) Improvements on global meteorological observations from the current Fengyun 3 satellites and beyond. *Int J Digit Earth* 5(3):251–265
- Yee MS, Walker JP, Rüdiger C et al (2017) A comparison of SMOS and AMSR2 soil moisture using representative sites of the OzNet monitoring network. *Remote Sens Environ* 195:297–312
- Zeng JY, Li Z, Chen Q et al (2015) Evaluation of remotely sensed and reanalysis soil moisture products over the Tibetan plateau using in-situ observations. *Remote Sens Environ* 163:91–110
- Zhang XF, Zhang TT, Zhou P et al (2017) Validation analysis of SMAP and AMSR2 soil moisture products over the United States using ground-based measurements. *Remote Sens* 9(2):104

Publisher's note Springer Nature remains neutral with regard to jurisdictional claims in published maps and institutional affiliations.